2011 9th IEEE International Conference on
Control and Automation (ICCA)
Santiago, Chile, December 19-21, 2011

A Fuzzy PD-PI Control Strategy to Track the Voltage References of Photovoltaic Arrays

Nilton E. M. Moçambique, Ricardo Q. Machado, Vilma A. Oliveira

Abstract— **In this paper, a fuzzy PD plus a PI controller structure for a photovoltaic PV system is presented. The controller tracks a voltage reference given by the perturb and observe P&O maximum power point tracking (MPPT) algorithm. The main drawback of the P&O MPPT algorithm is that at steady state the operating point oscillates around the maximum power point (MPP). The feedback control law proposed in this paper to track the references for a PV array connected to a DC-DC converter improves the P&O MPPT performance. Simulations under different environment conditions are provided to confirm the efficiency of the proposed approach.**

Index Terms— **PV systems, DC-DC converter, maximum power point tracking, fuzzy control.**

I. INTRODUCTION

Nowadays, the increasing global policies for alternative sources of energy have promoted the growth of the use of photovoltaic (PV) systems. As a result, the price per watt generated by PV systems is rapidly falling year by year stimulating a wide adoption including by developing countries [1].

A PV system uses the solar irradiation to convert into electrical energy. The solar irradiation which increases with the altitude is the total amount of solar energy accumulated in an area over time. During the day, the solar intensity varies sinusoidally with amplitude and phase varying according to the seasonal cycle [2]. A PV system is formed by PV cells which are connected in series and parallels to form modules, panels or arrays. In order to effectively analyze, simulate and implement PV applications, it is necessary a model to distinguish and quantify the influence of all significant factors [3]. Although, electrical, thermal, solar spectral and optical effects must be included in a PV model, it also must be practical and simple for common tasks in power systems [4], such as power flow, harmonic and sensitivity analysis and load matching [5].

It is desirable to draw the maximum power from the photovoltaic source and the converters should track continuously the maximum power point (MPP) using a maximum power point tracking (MPPT). Several MPPT algorithms were developed [6], [7] and [8]. A comparison of 19 different MPPT techniques is presented in [9]. However, the perturb and observe method P&O is the most simple method and also a low-cost implementation method. However, the solution given oscillates around the MPP in steady state and the method fails under rapidly changing atmospheric conditions [6]. In this paper is analyzed, simulated and implemented a photovoltaic circuit with a step up nonisolated (boost) converter operating in a continuous-conduction mode using a P&O method to establish the reference voltage of a feedback control system with a fuzzy PD-PI controller.

N. E. M. Moçambique is with the Department of Electrical Engineering, University of São Paulo, niltonmocambique@gmail.com

R. Q. Machado is with the Department of Electrical Engineering, University of São Paulo, rquadros@sc.usp.br

V. A. Oliveira is with the Department of Electrical Engineering, University of São Paulo, vilma@sc.usp.br

II. PV MODEL

A. Photovoltaic Cell Model

A PV cell basically is a silicon p-n junction that when exposed to light releases electrons around a closed electrical circuit [8]. The rate of electrons generated depends on the flux of incident light and the capacity of absorption of the silicon [4].

The generalized model of a PV cell consists of a light generated current source (I_{pv}), a series and shunt resistances (R_s and R_p, respectively), and two diodes (D_1 and D_2) representing the effect of the recombination of carriers [7], see Fig. 1. The shunt resistance R_s affects drastically the cell short-circuit current (I_{sc}) while R_p plays an important role on the cell open-circuit voltage (V_{oc}). However, the model circuit parameters are difficult to obtain and a single model diode shown in Fig. 2 is preferred. This model ensure simplicity and accuracy and is used by several authors [4], [6], [8], [10]–[12]. In general, PV cells with similar

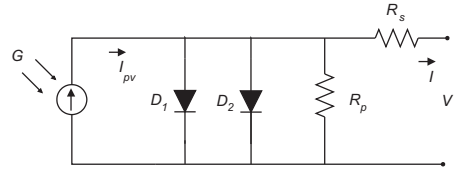

Fig. 1. Generalized model of solar cell.

characteristics are connected in series and encapsulated to form modules and arrays. If the module or array is evenly illuminated the resulting model is qualitatively the same as a single cell.

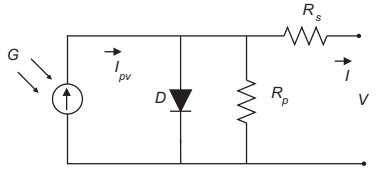

Fig. 2. Equivalent model of a practical PV cell.

978-1-4577-1476-4/11/$26.00 ©2011 IEEE

B. Photovoltaic Module Model

The model PV array adopted in this paper is presented in [4], and has the main advantages: all the required parameters are available by the manufacturer data sheets; it is an easy and effective model for the simulation of photovoltaic devices with power converters and guarantee that adjusted I-V (current vs. voltage) curve and P-V (power vs. voltage) curve matches experimental data in order to obtain the maximum power point (MPP). The $I-V$ characteristics of a photovoltaic module is given by,

$$I = I_{pv} - I_0 \left[\exp\left(\frac{V + R_s I}{V_t a} \right) - 1 \right] - \frac{V + R_s I}{R_p} \quad (1)$$

where I_{pv} is the light induced current, I_0 is the diode saturation current, a is the diode ideality factor, R_s is the equivalent series resistance of the array and R_p is the equivalent parallel resistance, $V_t = N_s kT/q$ is the thermal voltage of the array with N_s cells connected in series. If the module is composed of N_p parallel connections of cells, the PV and saturation currents are expressed as $I_{pv} = I_{pv,cell} N_p$ and $I_0 = I_{0,cell} N_p$, respectively. The current I_{pv} depends on the irradiance level G and on the array temperature T while I_0 depends only on the temperature T [6].

The $I-V$ curve in Fig. 3 exhibits the nonlinear relationship between the current I and the voltage V and the *remarkable points* of MPP (V_{mp}, I_{mp}).

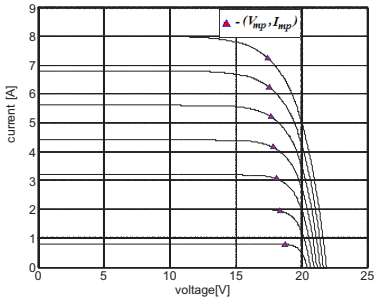

Fig. 3. Characteristic $I-V$ curve of KC130TM PV module for different levels of the irradiance and the remarkable points of MPP (V_{mp}, I_{mp}).

III. MPPT - PERTURB AND OBSERVE METHOD

The *P&O* MPPT algorithm is based on the following procedure: perturb the operating voltage in a given direction and observe if the power drawn by the PV array increase or decrease. If the power increases, then keep perturbing in the same direction, otherwise, perturb in the reverse direction, see Fig. 4. The algorithm does not stop even when MPP is reached, consequently, the voltage oscillates around the MPP. The oscillation can be minimized by reducing the perturbation step size. On the other hand, the smaller is the perturbation, the slower is the *P&O* method, reducing the efficiency during cloudy days [6]. To solve this problem, a varying perturbation step size is used such that the step size becomes smaller toward the MPP [9].

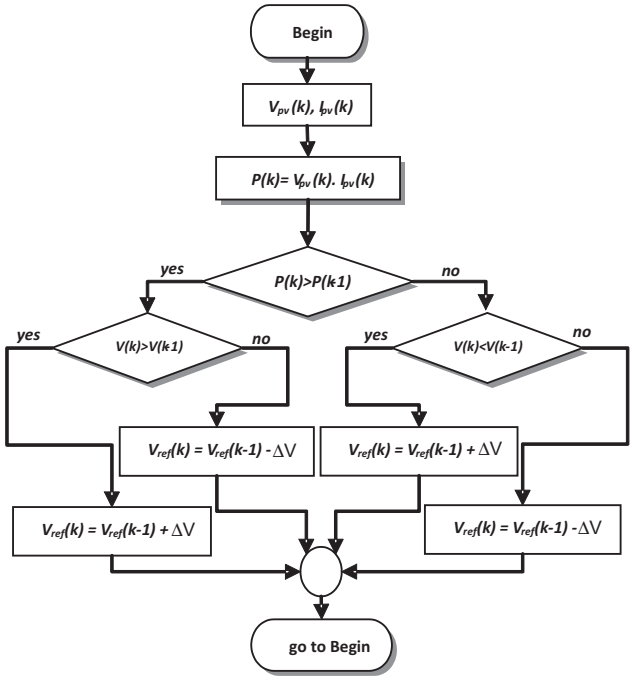

Fig. 4. *P&O* MPPT algorithm.

IV. LINEARIZED AVERAGE STATE SPACE EQUATIONS FOR A DC-DC CONVERTER

The goal of the following analysis is to find a small signal transfer function $\tilde{y}(s)/\tilde{d}(s)$ of the boost converter shown in Fig. 5, where $\tilde{y}$ and $\tilde{d}$ are small perturbations near the MPP in the PV output voltage y and switching duty-cycle d, respectively [13]. With the converter operating in a continuous-conduction mode, there are only two possible states: one state is when the switch is on and the other is when the switch is off.

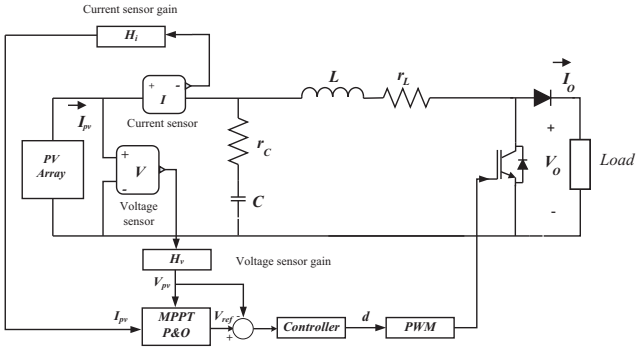

Fig. 5. Step up converter with control.

For the boost converter modeling, the effect of parasitic elements like the resistance of the switch in ON state (r_{ON}), series inductor resistance (r_L) and series capacitor resistance (r_C) are considered to better represent a practical converter [10]. Let $i_p v$ be the input current, corresponding to the current at the MPP, T_s the switching period, L the inductance and C the capacitance of the input filter and R the

load resistance suplied by the boost converter. Applying the Kirchhoff's current and voltage laws in the step up converter showed in Fig. 5 for the period dT_s it results

$$\begin{aligned}\frac{dv_C}{d_t} &= -\frac{i_L}{C}+\frac{i_{pv}}{C}\\ \frac{di_L}{d_t} &= \frac{v_C}{L}-\frac{(r_C+r_L+r_{ON})}{L}i_L+\frac{r_C}{L}i_{pv}\end{aligned} \tag{2}$$

In matrix form, defining $[x_1\ x_2]^T=[v_C\ i_L]^T$, (2) becomes

$$\dot{x}=A_1x+B_1i_{pv} \tag{3}$$

with

$$A_1=\begin{bmatrix}0 & -\frac{1}{C}\\ \frac{1}{L} & -\frac{(r_C+r_L+r_{ON})}{L}\end{bmatrix},\ B_1=\begin{bmatrix}\frac{1}{C}\\ \frac{r_C}{L}\end{bmatrix}.$$

Similarly, for the period $(1-d)T_s$ it results,

$$\dot{x}=A_2x+B_2i_{pv} \tag{4}$$

with

$$A_2=\begin{bmatrix}0 & -\frac{1}{C}\\ \frac{1}{L} & -\frac{(r_C+r_L+R)}{L}\end{bmatrix},\ B_2=\begin{bmatrix}\frac{1}{C}\\ \frac{r_C}{L}\end{bmatrix}.$$

The PV output voltage for both ON and OFF circuit states is given by $y=Cx+Di_{pv}$ with

$$C=[1\ -r_C],\ D=r_C. \tag{5}$$

In order to produce an average description of the step-up converter over a switching period, (3), (4) and (5) corresponding to the ON-OFF states are time weighted and averaged, resulting

$$\begin{aligned}\dot{x} &= [A_1d+A_2(1-d)]\,x+[B_1d+B_2(1-d)]\,i_{pv}\\ y &= [C_1d+C_2(1-d)]\,x+[D_1d+D_2(1-d)]\,i_{pv}.\end{aligned} \tag{6}$$

As $B_1=B_2, C_1=C_2, D_1=D_2$, it results

$$\begin{aligned}\dot{x}&=[A_1d+A_2(1-d)]\,x+[B_2]\,i_{pv}\\ y&=[C_2]\,x+[D_2]\,i_{pv}.\end{aligned} \tag{7}$$

Consider the DC steady-state with small AC perturbations as [13]

$$\begin{aligned}x &= \bar{X}+\tilde{x}\\ d &= D+\tilde{d}\\ i_{pv} &= I_{pv}+\tilde{i}_{pv}\\ y &= Y+\tilde{y},\end{aligned} \tag{8}$$

and assume that the perturbation $\tilde{i}_{pv}$ in the input current is zero. Replacing (8) in (7) and applying Laplace transform, the small signal transfer function of the PV-boost system can be obtained as

$$\frac{\tilde{y}(s)}{\tilde{d}(s)}=C_2\left[[sI-A]^{-1}[A_1-A_2]\right]X \tag{9}$$

where

$$X=-A^{-1}B_2I_{pv} \text{ with } A=A_1D+A_2(1-D).$$

V. FUZZY PD-PI CONTROLLER DESIGN

In order to control the power of the PV array, a feedback control law to work under small deviation of the MPP is proposed (see Fig. 6). Since the linearized plant is of second order, a first order controller will track effectively a step input. Consequently, a proportional and integral control would be a good choice. However, an improved performance can be achieved with the combination fuzzy PD plus PI.

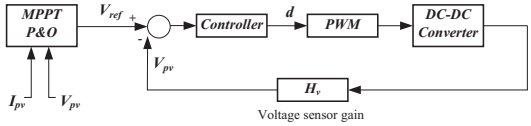

Fig. 6. Block diagram of the step-up DC-DC converter with control and reference generated by the MPPT.

A. Fuzzy PD-PI Controller design

The controller is obtained as a combination of a fuzzy PD plus the PI classical actions. The controller structure is showed in Fig. 7.

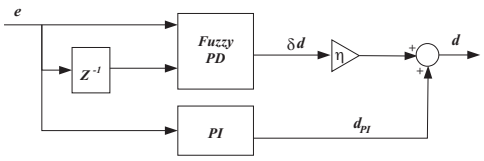

Fig. 7. Controller scheme for the DC-DC converter.

The inputs of the fuzzy controller are the error e and one level error difference Δe, given by

$$\begin{aligned}e(k)&=V_{ref}-V_{pv}\\ \Delta e(k)&=e(k)-e(k-1)\end{aligned} \tag{10}$$

where k is the actual time instant, V_{ref} is the reference voltage which is provided by the MPPT algorithm and V_{pv} is the actual PV voltage. The output of the fuzzy PD controller is the change of the duty cycle δd and can be expressed approximately as [14]

$$\eta\delta d(k)=\frac{e(k)}{n_e}+\frac{\Delta e(k)}{n_{\Delta e}} \tag{11}$$

where $\delta d(k)$ is the inferred change of duty cycle by the fuzzy controller, η is a weighting gain, n_e and $n_{\Delta e}$ are the normalization factors for e and for Δe, respectively. The values of the normalization factors depend on the converter used.

The membership functions were chosen with triangular and trapezoidal shape, because they have a simpler parametric representation and require less hardware memory [15]. The fuzzy sets for both the inputs and output are (positive), NE (negative), ZE (zero) as shown in Fig. 8. The construction of control rules to relate the fuzzy input to the fuzzy output depends on the knowledge base of the system dynamics. The control rules proposed is presented in Table I.

After fuzzifiying the input pair of values (e and Δe), takes place the inference procedure, resulting in a fuzzy output region which is related with the process output δd. Basically, the inference procedure consists of the following steps: 1) find all rules activated, 2) determine the fuzzy output for each rule by applying the generalized modus-pones rule (i.e . if e is < linguistic variable> and Δe is < linguistic variable> then δd is < linguistic variable >), and at last, 3) aggregate all fuzzy rule outputs.

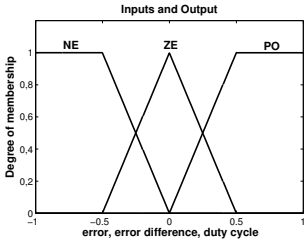

Fig. 8. Membership functions of the input-output variables.

TABLE I
RULE BASE FOR THE FUZZY PD SYSTEM

		e		
	δd	Negative	Zero	Positive
Δe	Negative	Positive	Zero	Negative
	Zero	Positive	Zero	Negative
	Positive	Positive	Zero	Negative

The *and* Boolean operation in each rule is implemented with the function *product* and the *inference* operation with the *minimum* function. The aggregation of all fuzzy outputs regions is implemented with the function *maximum*. The defuzzification was performed by the centroid method, as follows

$$\delta d = \frac{\sum_{k=1}^{N} \mu(V_k)\ V_k}{\sum_{k=1}^{N} \mu(V_k)} \tag{12}$$

where μ is the degree of membership, N is the number of discretized elements and V_k is a crisp element in the universe of discourse. Fig. 9 shows the resulting surface.

In differential equation form, the duty cycle at the k_{th} time using the fuzzy PD-PI controller is given by

$$d(k) = d_{PI}(k) + \eta\ \delta d(k). \tag{13}$$

VI. SIMULATIONS RESULTS

In this section simulation results for two KC130TM solar modules for 260W are presented. The *fuzzy* toolbox of $MatLab^{TM}$ was used to implement the fuzzy controller. The results were obtained by simulating the system model shown in Fig. 5 using the SimPowerSystem of Simulink $Matlab^{TM}$ software.

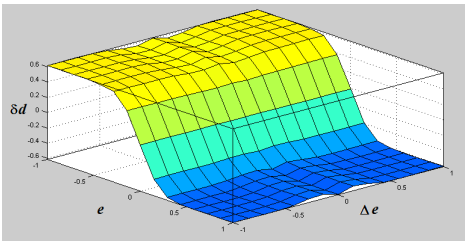

Fig. 9. Fuzzy system surface.

Even though the consequent membership functions were linguistic variables, the high-speed of decision making was ensured since were used only three fuzzy sets and triangular shapes per each input and output variables.

Table II presents the parameters of the $I-V$ characteristic of the photovoltaic module described in (1) for two KC130TM solar modules connected in series at standard test conditions. The parameters R_s and R_p are obtained with the method given in [4]. The remaining are provided by the manufacture datasheet. The parameters of the boost converter are shown in Table III. The values of the parameters D and L were obtained via the approach given in [16].

To obtain the PI controller gains, the PV - boost system model (9) was used in the *sisotool* ($MatLab^{TM}$ toolbox). The PI parameters proportional and integral gains found are showed in Table IV.

TABLE II
PARAMETERS OF THE ADJUSTED SOLAR MODEL

$V_{mp}[V]$	35.2
$I_{mp}[A]$	7.39
$P_{max}[W]$	4260.128
$I_{o,n}[A]$	3.598×10^{-9}
$V_{ocn}[V]$	43.8
$I_{pv}[A]$	8.0378
A	1.1
$R_p[\Omega]$	176.272
$R_s[\Omega]$	0.180

TABLE III
PARAMETERS OF THE BOOST CONVERTER

L $[mH]$	r_L $[\Omega]$	C $[\mu F]$	r_C $[\Omega]$	D	V_0 $[V]$
5	0.3	1000	0.25	0.76	150

TABLE IV
PI GAINS FOR THE BOOST CONVERTER

Bandwidth (Hz)	Phase - margin (degree)	K_p	K_i
1000	60	-20.7	-2246

For comparison purposes, results for a constant V_{ref} with the PI controller and the fuzzy PD-PI controller are showed in Fig 10. The fuzzy PD-PI controller responses resemble the conventional PI controller responses but with a better

performance. Simulations results for the references given by the P&O MPPT are showed for fixed step, varying step, rapidly temperature and irradiance changes and load disturbance.

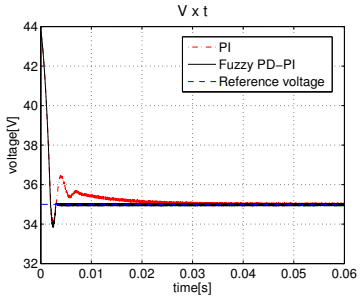

Fig. 10. PV voltage time responses for $V_{ref} = 35V$ using a PI controller (dashed line) and a fuzzy PD-PI controller (solid line) with $T_s = 1\mu s$, *ripple* = 0.2V.

A. Establishing initial conditions

In practice, the voltage gain of the boost converter decreases as the duty ratio approaches the unity [13]. In general, the maximum voltage gain is limited to the interval [5 6]. Consequently, although the fuzzy PD-PI was designed to track several reference voltages in the neighborhood of the MPP, the farther is the reference from the MPP, the larger will be the overshoot and the settling time. In this case, the control is effective but it is not efficient.

As a result, it is necessary to estimate the initial voltage on the capacitor and the initial current on the inductor, approximating the simulation to the real conditions. Admitting the gate of the converter disconnected, and after a large period of time (more than 6 times of the time constant) the capacitor voltage is the voltage of the PV open circuit (V_{oc}) and the current in the inductor is zero. We take V_{oc} and zero as the initial conditions.

B. Choosing the sampling interval T_α

To choose the sampling interval T_α used by the P&O MPPT algorithm, one should consider the following. The sampling interval should be set higher than a threshold value to ensure that the PV system stabilizes and to reduce the number of oscillations around the MPP in steady state, before the next measurement of both voltage and current. The threshold time is approximately by

$$T_\epsilon \cong -\frac{\sqrt{LC}}{\zeta} ln(\epsilon) \tag{14}$$

as in [6].

Commonly $\epsilon = 0.1$ is a reasonable value to ensure that the transient is over [6]. And the damping ratio ζ is given by

$$\zeta = \frac{1}{2}\frac{I_{mpp}}{V_{mpp}}\sqrt{\frac{L}{C}} + \left(\frac{r_C + r_L}{2}\right)\sqrt{\frac{C}{L}}. \tag{15}$$

Using Tables I and II results $\zeta = 0.3130$ and $T_{0.1} = 0.0165$ seconds yielding $T_\alpha \geq T_{0.1}$.

C. Converter dynamics

Starting the initial voltage on the capacitor equal to the voltage of the PV open circuit (V_{oc}) and with no initial current on the inductor, the P&O MPPT algorithm initially perturbs (by increasing) the reference voltage of the fuzzy PD - PI control and "observes" the power drawn from the PV array decreasing, this mean that the reference voltage has moved away from the MPP, thus it decreases the reference voltage and the MPP is reached. At this moment, the system starts the steady state oscillating around the MPP as shown in Fig. 11 with a fixed step of 1.0V and with a varying step in Fig.12. The results thus showed that the fuzzy PD-PI controller has a good performance, with low overshoot and fast settling time, taking the system rapidly to the steady-state. These advantage permits a T_ϵ smaller than 0.0165 seconds without compromising the MPPT efficiency and providing a faster responses.

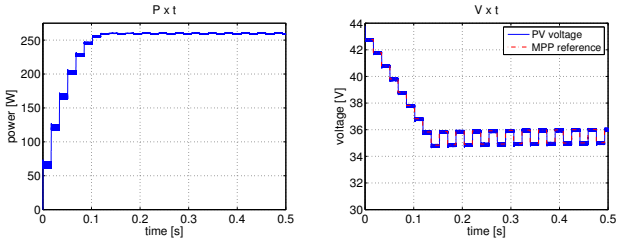

(a) (b)

Fig. 11. Time domain simulations at $G = 1000W/m^2$ $T = 298.15K$ and $T_\alpha = 0.017s$ with fixed step = 1.0 V. (a) power and (b) voltage responses.

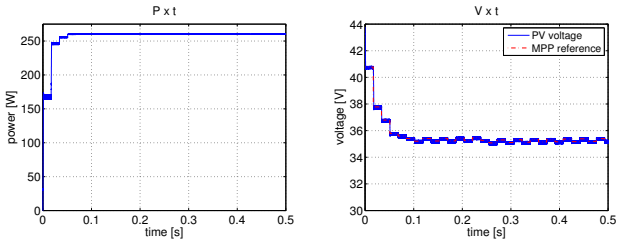

(a) (b)

Fig. 12. Time domain simulations at $G = 1000W/m^2$, $T = 298.15K$ and $T_\alpha = 0.017s$ with a varying step of [5.0 1.0 0.5]V. (a) power and (b) voltage responses.

D. Rapidly irradiance and temperature conditions changes

In cloudy days normally occurs fast changing in the irradiance, this may confuse the P&O MPPT algorithm and, decrease the MPPT efficiency. This situation only happens if the irradiance variation ΔG produces a power variation ΔP_G larger than the power variation due to the step of the MPPT ΔP_{step} [6]. The simulations shown in Fig. 13 take into account these factors. Note that ΔG affects dramatically the ΔP, even a large ΔT has a slight influence ΔP at steady state.

E. Load disturbance rejection

The PV system presented in this paper was designed to work as a battery charger. However, in many applications of distributed generation, the PV system is connected to a grid by an inverter. In order to analyze the robustness of the fuzzy PD - PI controller, in Fig.15 it is shown the simulation of the PV system of Fig.5 connected to a DC link of 260W plus a voltage source inverter. To simplify, the DC link model is implemented as a DC source plus an AC disturbance of $\pm$ 10% of the DC link rated voltage.

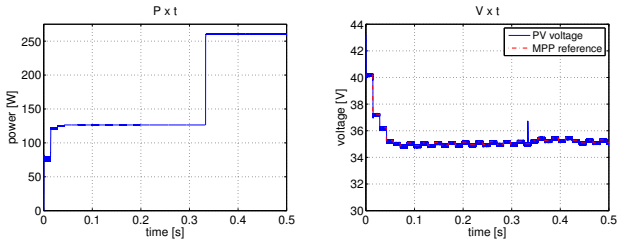

(a) (b)

Fig. 13. Rapidly irradiance changes at time=0.4s, $G = 500W/m^2$ (before 0.4s) and $G = 1000W/m^2$ (after 0.4s), T=298.15 K, $T_\alpha = 0.017s$. (a) power and (b) voltage responses.

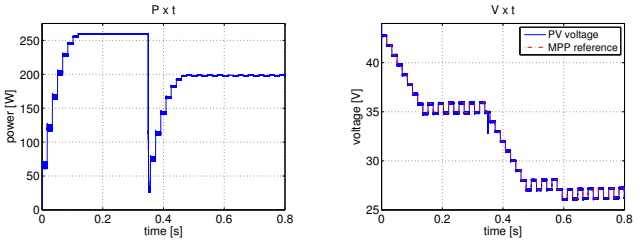

(a) (b)

Fig. 14. Rapidly temperature changes at time=0.35s, t= 25° C (before 0.35s) and t= 75° C (after 0.35s), $G = 1000W/m^2$ K, $T_\alpha = 0.017s$. (a) power and (b) voltage responses.

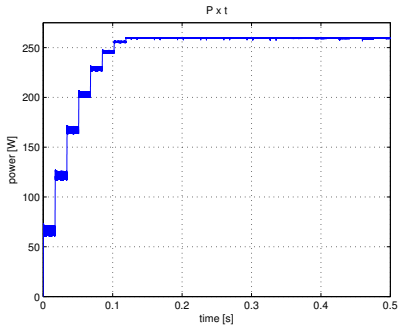

Fig. 15. Power response simulation of a PV system for a voltage source ($V_{ac} = 40V, f_{ac} = 120Hz$) in series with the DC link ($V_o = 150V$), at $G = 1000W/m^2$, $T = 298.15K$, $T_\alpha = 0.017s$.

VII. CONCLUSION

In this paper simulations of PV system were presented considering some of the possible situations in which the converter will operate. The results confirm that by applying a feedback control to track the PV array voltage references, the performance of the MPPT P&O algorithm is improved. Smaller sampling interval, lower overshoot and fast settling time to fast irradiance changes are obtained. The results obtained and the considerations drawn can be extended to any other nonlinear controller and converter topology in PV system applications.

REFERENCES

[1] J. Donovan. (2011, May) Fundamentals of solar: Grid-connected. Texas Instruments. [Online]. Available: http://seminar2.techonline.com/fundamentals/solar1/player.html

[2] G. Musser, "A solar detective story: explaining how power output varies hour by hour," Scientific American, july 2010. [Online]. Available: http://blogs.scientificamerican.com/solar-at-home/2010/07/30/

[3] D. L. King, W. E. Boyson, and J. A. Kratochvil, "Photovoltaic array performance model," Sandia National Laboratories, august 2004. [Online]. Available: http://photovoltaics.sandia.gov/docs/PDF/King%20SAND.pdf

[4] M. Villalva, J. R. Gazoli, and E. R. Filho, "Comprehensive approach to modeling and simulation of photovoltaic arrays," *IEEE Transactions on Power Electronics*, vol. 24, no. 5, pp. 1198–1208, 2009.

[5] E. I. Ortiz-Rivera and F. Peng, "Analytical model for a photovoltaic module using the electrical characteristics provided by the manufacturer data sheet," *IEEE Power Electronics Specialists Conference*, pp. 2087–2091, june 2005.

[6] N. Femia, G. Petrone, G. Spagnuolo, and M. Vitelli, "Optimization of perturb and observe maximum power point tracking method," *IEEE Transactions on Power Electronics*, vol. 20, no. 4, pp. 963–973, 2005.

[7] E. Ortiz-Rivera and F. Peng, "A novel method to estimate the maximum power for a photovoltaic inverter system," in *35th Annual IEEE Power Electronics Specialists Conference*, vol. 3, june 2004, pp. 2065–2069.

[8] C. Rodriguez and G. Amaratunga, "Analytic solution to the photovoltaic maximum power point problem," *IEEE Transactions on Circuits and Systems - I: Regular Papers*, vol. 54, no. 9, pp. 2054–2060, 2007.

[9] T. Esram and P. L. Chapman, "Comparison of photovoltaic array maximum power point tracking techniques," *IEEE Transactions on Energy Conversion*, vol. 22, no. 2, pp. 439–449, 2007.

[10] A. Masoum, F. Padovan, and M. Masoum, "Impact of partial shading on voltage - and current based maximum power point tracking of solar modules," in *IEEE Power and Energy Society General Meeting*, july 2010, pp. 1–5.

[11] R. Ramaprabha and B. Mathur, "Modelling and simulation of solar PV array under partial shaded conditions," in *IEEE International Conference on Sustainable Energy Technologies*, nov. 2008, pp. 7–11.

[12] H. Patel and V. Agarwal, "Matlab - based modeling to study the effects of partial shading on PV array characteristics," *IEEE Transactions on Energy Conversion*, vol. 23, no. 1, pp. 302–310, 2008.

[13] N. Mohan, T. M. Undeland, and W. Robbins, *Power Electronics: Converters, Application and Design*, 2nd ed. John Willey, 1995.

[14] U. Yaragatti, A. Rajkiran, and B. Shreesha, "A novel method of fuzzy controlled maximum power point tracking in photovoltaic systems," in *IEEE International Conference on Industrial Technology*, dec. 2005, pp. 1421–1426.

[15] M. Di Piazza, M. Pucci, A. Ragusa, and G. Vitale, "Fuzzified PI voltage control for boost converters in multi-string PV plants," in *IEEE Industrial Electronics, IEC Annual Conference of Industrial Electronics*, nov. 2008, pp. 2338–2345.

[16] E. Ortiz-Rivera, "Maximum power point tracking using the optimal duty ratio for dc-dc converters and load matching in photovoltaic applications," in *IEEE Applied Power Electronics Conference and Exposition*, feb. 2008, pp. 987 –991.